HHS Public Access

Author manuscript

J Control Release. Author manuscript; available in PMC 2019 April 25.

Published in final edited form as:

J Control Release. 2018 October 10; 287: 235–246. doi:10.1016/j.jconrel.2018.08.021.

TNFα gene silencing mediated by orally targeted nanoparticles combined with interleukin-22 for synergistic combination therapy of ulcerative colitis

Bo Xiao[a,b,*,1], **Qiubing Chen**[a,1], **Zhan Zhang**[b], **Lixin Wang**[b,c], **Yuejun Kang**[a], **Timothy Denning**[b], and **Didier Merlin**[b,c]

[a]Institute for Clean Energy and Advanced Materials, Faculty for Materials and Energy, Southwest University, Beibei, Chongqing 400715, PR China

[b]Institute for Biomedical Sciences, Center for Diagnostics and Therapeutics, Digestive Disease Research Group, Georgia State University, Atlanta, GA 30302, USA

[c]Atlanta Veterans Affairs Medical Center, Decatur, GA 30033, USA

Abstract

Pro-resolving factors that are critical for colonic epithelial restitution were down-regulated during the treatment with inhibitor of pro-inflammatory cytokines (*e.g.*, anti-TNFα antibody) in ulcerative colitis (UC) therapy. We hypothesized that increased amounts of factors such as interleukin-22 (IL-22) during the therapeutic inhibition of TNFα could facilitate the resolution of intestinal inflammation. As combination therapy is an emerging strategy for UC treatment, we attempt to treat established UC based on the combination of TNFα siRNA (siTNF) and IL-22. Initially, we loaded siTNF into galactosylated polymeric nanoparticles (NPs). The resultant Gal-siTNF-NPs had a desirable average diameter (~261 nm), a narrow size distribution and a slightly negative surface charge (~−6mV). These NPs successfully mediated the targeted delivery of siTNF to macrophages and efficiently inhibited the expression of TNFα. Meanwhile, IL-22 could obviously accelerate mucosal healing. More importantly, oral administration of Gal-siTNF-NPs plus IL-22 embedded in a hydrogel (chitosan/alginate) showed much stronger capacities to down-regulate the expression of pro-inflammatory factors and promote mucosal healing. This formulation also yielded a much better therapeutic efficacy against UC in a mouse model compared to hydrogel loaded with Gal-siTNF-NPs or IL-22 alone. Our results strongly demonstrate that Gal-siTNF-NP/IL-22-embedded hydrogel can target to inflamed colon, and co-deliver siTNF and IL-22 to boost the effects of either monotherapy, which may become a promising oral drug formulation and enable targeted combination therapy of UC.

[*]Corresponding author at: Institute for Clean Energy and Advanced Materials, Faculty for Materials and Energy, Southwest University, Beibei, Chongqing 400715, PR China. hustboxiao@gmail.com (B. Xiao).

[1]These authors are contributed equally to this work.

Appendix A. Supplementary data

Supplementary data to this article can be found online at https://doi.org/10.1016/j.jconrel.2018.08.021.

Keywords

TNFα silencing; Interleukin-22; Oral administration; Targeted nanoparticle; Ulcerative colitis; Combination therapy

1. Introduction

Ulcerative colitis (UC) is a chronic and relapsing inflammatory disease in distal bowel, which is characterized by uncontrolled intestinal inflammation and disruption of colonic epithelial layer [1, 2]. It affects several million individuals worldwide and its prevalence rate rises sharply in low-incidence countries [3]. The current medical treatments for UC mainly depend on the usage of aminosalicylates, corticosteroids and immunosuppressive drugs [4, 5]. However, these drugs are usually administered at high doses *via* intravenous injection, leading to serious adverse effects (*e.g.*, diarrhea, osteoporosis and infection) [6, 7]. Therefore, it is critically important to develop alternative drug formulations with high therapeutic efficacies and low side effects.

Macrophages contribute to the onset and progression of UC by producing a large amount of pro-inflammatory cytokines, such as tumor necrosis factor alpha (TNFα) [8, 9]. Although anti-TNFα monoclonal antibody infliximab has yielded promising therapeutic outcomes in clinical UC treatment, it suffers from several major limitations, including serious infections, auto-immunity to antibodies and high cost [10]. Recently, RNA interference (RNAi) has gained considerable attention for its ability to efficiently and specifically down-regulate TNFα expression in macrophages [11, 12]. However, siRNAs are anionic, easily degradable and hydrophilic, complicating their internalization into cells; moreover, they are lack of targeting capacity [13]. Thus, the success of RNAi relies heavily on the application of siRNA carriers. Various carriers have been employed for siRNA delivery, such as micelles, liposomes and nanoparticles (NPs) [12, 14, 15]. Among these options, polymeric NPs have attracted much attention owing to their high siRNA encapsulation efficiency, controlled siRNA release capacity and ease of surface functionalization [16]. Moreover, it was noticed that targeted delivery of siRNAs to specific cells mediated by active ligands could further improve the therapeutic efficacy of NPs in UC treatment [17]. Macrophage galactose type lectin (MGL), a ~42kDa type II transmembrane glycoprotein that contains a galactose-recognition domain, is dramatically overexpressed on the surface of activated macrophages under inflammatory conditions [18]. This lectin can specifically bind to NPs with galactose residues, resulting in rapid internalization into membrane-bound vesicles [19]. Based on these findings, galactose is expected to be an excellent ligand for macrophage-targeted drug delivery. The conjugation of galactose to the surfaces of various carriers, such as chitosan complexes, polyanhydride NPs and low-density lipoprotein carriers, has been shown to provide selective macrophage targeting and improve cellular uptake [20–22].

Since the treatment goals of UC in clinic are to both control inflammation and achieve mucosal healing [23, 24], combination therapy based on multiple drugs has been proposed as a potential strategy [25, 26]. Interleukin-22 (IL-22) is a pro-healing cytokine that has numerous benefits to restore intestinal homeostasis: (1) It induces the survival, proliferation

and reconstitution of epithelial cells, preventing microbiota from further penetrating into the colonic tissues [27, 28]; (2) It facilitates regeneration of goblet cells and increases production of mucus-associated proteins, which form the essential static external barrier that separates intestinal flora from intestinal epithelial cells [29]; (3) It stimulates intestinal epithelial cells and Paneth cells to express and secret a large amount of antimicrobial peptides, which sequester or kill invading pathogens [29, 30]. In recent preclinical studies based on IL-22-deficient mice or wild-type mice subjected to dextran sulfate sodium (DSS)-induced UC, treatment with a IL-22-neutralizing antibody induced severe weight loss, augmented damage in the colonic epithelial layer and aggravated inflammation in the colon [30–32]. Conversely, overexpression of IL-22 in T cell receptor-alpha-deficient mice reduced the colonic thickness and disease score during DSS-induced UC [29]. Therefore, it can be speculated that IL-22 is a key therapeutic molecule to improve intestinal healing in patients with UC.

Poly(lactic acid/glycolic acid) (PLGA) is an FDA-approved biodegradable polymer that can efficiently encapsulate hydrophilic drugs (*e.g.,* plasmids, siRNAs and proteins) [33]. Thus, it has been widely used as a drug carrier matrix by our group and others [16, 34]. In the present study, we fabricated galactose-functionalized TNFα siRNA-loaded PLGA NPs (Gal-siTNF-NPs), and characterized their physicochemical properties, macrophage-targeted capacities and anti-inflammation activities. In the meantime, we studied the mucosal healing capacity of IL-22. To enable the co-delivery of Gal-siTNF-NPs and IL-22 to colonic lumen, we embedded both agents in a hydrogel and further evaluated their synergistic therapeutic effects on the basis of a DSS-induced mouse model of UC.

2. Materials and methods

2.1. Materials

PLGA with an equal molar ratio of lactide and glycolide (molecular weight = 38–54 kg/mol), poly(vinyl alcohol) (PVA, 86–89% hydrolyzed, low molecular weight), spermidine, chitosan, sodium nitrite, lactobionic acid (LA), 1-ethyl-3-(3-dimethylaminopropyl)-carbodiimide (EDC), *N*-hydroxysuccinimide (NHS), 2-(*N*-morpholino) ethanesulfonic acid sodium salt (MES), alginate, dichloromethane (DCM), dimethyl sulfoxide, O-dianisidine hydrochloride, Triton X-100 and lipopolysaccharide (LPS) were purchased from Sigma-Aldrich (St. Louis, MO). Chitosan was purified before use, and it was depolymerized using sodium nitrite. Viscosity-average molecular weights of the original chitosan and the depolymerized chitosan were determined as 246 kDa and 18 kDa, respectively. The depolymerized chitosan was used in the NP preparation process. Paraformaldehyde stock solution (16%) was from Electron Microscopy Science (Hatfield, PA). Oligofectamine™ (OF) transfection reagent, 3-(4,5-dimethylthiazol-2-yl)-2,5-diphenyl tetrazolium bromide (MTT), 4′,6-diamidino-2-phenyl-indole dihydrochloride (DAPI), 1,1′-dioctadecyl-3,3,3′,3′-tetramethylindotricarbocyanine iodide (DiR) and FITC fluorescently tagged siRNA (FITC-siRNA) were supplied from Invitrogen (Eugene, OR). TNFα siRNA (siTNF) was purchased from Santa Cruz Biotechnology (Santa Cruz, CA). Recombinant human IL-22 and recombinant mouse IL-22 were purchased from R&D systems (Minneapolis, MN). Anti-murine TNFα antibody was kindly provided by Janssen Biotech (Horsham, PA). DSS

(36–50 kDa) was obtained from MP Biomedicals (Aurora, OH). Buffered formalin (10%) was supplied by EMD Millipore (Billerica, MA). Hematoxylin and eosin were from Richard-Allan Scientific (Kalamazoo, MI). All commercial products were used without further purification.

2.2. Anti-TNFα antibody treatment of IL10$^{-/-}$ mice

IL10$^{-/-}$ female mice (3 weeks of age) were obtained from The Jackson Laboratory. The animal experiments were approved by Georgia State University Institutional Animal Care and Use Committee. They developed colitis on a time-dependent manner, and they were treated twice a week from 4 to 14 weeks of age by intraperitoneal injection of equal volumes of either phosphate-buffered saline (PBS) or anti-murine TNFα antibody (10mg/kg mice, 200–250 μg/mice). Mice were euthanized at 14 weeks of age, and total RNA were extracted from colon tissues using RNeasy Plus Mini Kit (Qiagen, Valencia, CA). Thereafter, cDNA was synthesized using Maxima first strand cDNA synthesis kit (Fermentas, Glen Burnie, MD). Consequently, the TNFα mRNA expression levels were quantified by quantitative reverse-transcription polymerase chain reaction (RT-PCR) using Maxima® SYBR Green/ROX qPCR Master Mix (Fermentas). Sequences of all the primers used in RT-PCR studies are presented in Table S1.

2.3. Fabrication of Gal-siTNF-NPs

siTNF-loaded NPs were produced by a double emulsion-solvent evaporation method. Briefly, siRNA was dissolved in RNase-free water, and further complexed with spermidine at N/P ratio (molar ratio of the triamine nitrogen to the polynucleotide phosphate) of 8:1 to form spermidine/siRNA complexes. PLGA (100 mg) was completely dissolved in DCM (2 mL). Subsequently, the inner aqueous solution (0.1 mL) was poured into the oil phase to form the first emulsion. PVA solutions (5%, *w/v*) with chitosan (0.3%, w/v) were prepared in diluted hydrochloric acid solution (0.1%, *v/v*). Addition of the first emulsion to 4 mL of PVA (5%, w/v)/chitosan (0.3%, w/v) solution and subsequent sonication (6 times, 10 s each time) of the whole mixture resulted in the formation of a double emulsion, and DCM was removed by a rotary evaporator (Yamato RE200, Santa Clara, CA). The formed NPs were obtained by centrifugation at 17,418*g* for 20 min, washed 3 times with deionized water, and re-suspended in threhalose solution (5%, *w/v*). Finally, NPs were dried in a lyophilizer at a temperature below −50 °C and a vacuum level of 0.05 mbar, and stored at −20 °C in airtight container. Depolymerized chitosan-coated NPs were designated as CS-coated NPs.

As to the further conjugation of LA, CS-coated NPs were dispersed in MES buffer (pH 5.5). The carboxyl group of LA was activated by EDC/NHS for 2 h, and this LA solution was added to CS-coated NP suspension. The resultant mixture was allowed to react at ambient temperature with stirring for 3 h. The final NPs were collected by centrifugation at 17,418*g* for 20 min, washed 3 times with deionized water, and resuspended in threhalose solution (5%, *w/v*). Finally, the resultant NPs were dried in a lyophilizer, and stored at −20 °C in airtight container.

2.4. Biocompatibility tests of NPs

Raw 264.7 macrophages and Colon-26 cells were cultured at a respective density of 2×10^4 and 8×10^3 cells/well in 96-well plates. After 24 or 48 h of exposure to NP suspensions, cells were incubated with 100 μL of MTT working solution at 37 °C for 3 h. This solution was prepared in serum-free medium with the MTT concentration of 0.5mg/mL. Subsequently, the media were discarded and 50 μL of dimethyl sulfoxide was added to each well prior to spectrophotometric measurements at 570 nm. Untreated cells were used as a negative control, whereas Triton X-100 (0.5%, *w/v*)-treated cells were used as a positive reference. In addition, OF/siRNA complexes were also used as a control here.

2.5. Visualization of cellular uptake profiles of NPs

Raw 264.7 macrophages were seeded in eight-chamber tissue culture glass slide (BD Falcon, Bedford, MA) at a density of 2×10^4 cells/well. After exposure to Gal-FITC-siRNA-NPs for 3 or 5h, cells were thoroughly rinsed with PBS to eliminate excess NPs, and fixed in paraformaldehyde (4%, *v*/v) for 20 min. Thereafter, nucleus was stained by DAPI for 5 min. Untreated cells were used as a negative control, whereas cells in the presence of OF/FITC-siRNA complexes were treated as a positive control. Images were acquired using FITC channel and DAPI channel on an Olympus fluorescence microscope equipped with a Hamamatsu Digital Camera ORCA-03G.

2.6. Quantification of cellular uptake efficiencies of NPs

Raw 264.7 macrophages were seeded in 12-well plates at a density of 1×10^5 cells/well. The medium was changed to serum-free medium containing various NPs or complexes. At predetermined time intervals (0, 1, 3 and 5 h), cells were thoroughly rinsed with PBS to eliminate excess NPs. Subsequently, the treated cells were harvested using trypsin, transferred to centrifuge tubes, and centrifuged at 1800*g* for 5 min. Upon removal of the supernatant, cells were re-suspended in flow cytometry (FCM) buffer. Analytical FCM was performed using the FITC channel on the FCM Canto™ (BD Biosciences), and a total of 5000 ungated cells were analyzed. Untreated cells were used as a negative control, whereas cells in the presence of OF/FITC-siRNA complexes were treated as a positive control.

2.7. In vitro gene silencing efficiencies of NPs

Raw 264.7 macrophages were seeded in 6-well plates at a density of 1×10^5 cells/well. After co-culture with NPs for 5h, cells were incubated in medium containing 10% FBS for 19, 43, 67 or 91 h. Thereafter, Raw 264.7 macrophages were stimulated with LPS (1 μg/mL) for 3 h. The processes for RNA extraction, cDNA synthesis and quantification of TNFα mRNA expression levels were the same as described in Section 2.2.

2.8. In vitro mucosal healing property of IL-22

Since the transepithelial barrier is critical for colon, we studied the mucosal healing effects of IL-22 on colonic barrier function *in vitro.* This assay was performed using electrical impedance sensing technology (ECIS, Applied BioPhysics, Troy, NY), and the ECIS model 1600R was used in the experiment. This system consisted of an 8-well culture dish (ECIS 8W1E plate), and Caco2-BBE cells were seeded in the culture dish at a density of 1×10^6/

well. Once cells reached confluence, an elevated current pulse (3 mA, 40 kHz, 30 s) was applied to wound the monolayer of Caco2-BBE cells. The wounding pulse was reflected by a sharp drop in resistance. Subsequently, the system was switched back to its normal operation to monitor the process of wound healing. After that, IL-22 with various concentrations (0, 50 and 100 ng/mL) was added to the wells.

2.9. Induction of UC mouse model and oral administration of drug formulations

FVB male mice (8 weeks of age, The Jackson Laboratory) were used in the animal experiments. All the animal experiments were approved by Georgia State University Institutional Animal Care and Use Committee. UC was induced by replacing their drinking water with a 3.0% (*w/v*) DSS solution for 7 days. To deliver various drugs to mice colonic lumen, we encapsulated them into a hydrogel comprised of chitosan and alginate at a weight ratio of 3:7 (detailed protocol available at http://www.natureprotocols.com/2009/09/03/a_method_to_target_bioactive_c.php), which have been commonly used for oral drug delivery in our previous studies [12, 16, 35–38]. Mice were treated with 20 μg/kg of siTNF and/or 50 μg/kg of IL-22 per day. Control mice were given water only. Mice were sacrificed by CO_2 euthanasia, and their spleen weight and colon length were measured. A small piece (50 mg) of colon was taken for MPO and RNA analysis, and the remaining colon was used for histopathological analysis.

2.10. Ex vivo imaging of drug formulations

To track the NP distribution in gastrointestinal tract (GIT) after oral administration, the near infrared dye DiR was employed as a fluorescence probe. Gal-DiR-NPs were fabricated by a single emulsion solvent evaporation technique, and the loading amount of DiR in Gal-DiR-NPs was quantified by a UV-Vis spectra method. UC mouse model was induced by DSS, and these mice were orally administered with Gal-DiR-NP-embedded hydrogel at a DiR concentration of 0.5 mg DiR/kg mice. After oral administration for 4, 8 and 24 h, mice were sacrificed to obtain GIT, and this GIT was imaged using an IVIS spectrum imaging system (PerkinElmer/Caliper LifeSciences, Hopkinton, MA).

2.11. In vivo cellular uptake profiles of NPs

UC mouse model was induced by DSS, and these mice were orally administered with FITC-siRNA-NP or Gal-FITC-siRNA-NP-embedded hydrogel (20 μg FITC-siRNA/kg mice). After 12 h of oral administration, mice were sacrificed by CO_2 euthanasia. Colon tissues were extracted, rinsed with PBS and embedded in Optimal Cutting Temperature compound. Colonic sections (5 μm) were stained with DAPI. Images were acquired using an Olympus microscope equipped with a Hamamatsu Digital Camera ORCA-03G.

To investigate the *in vivo* targeting property of NPs, mice with UC were orally administered with FITC-siRNA-NP- or Gal-FITC-siRNA-NP-embedded hydrogel (20 μg FITC-siRNA/kg mice). After 12 h, mice were euthanized by CO_2 euthanasia, and their spleen and colon were obtained. Isolation of splenocytes and lamina propria immune cells was carried out as described in our previous reports [39, 40]. Antibodies used for analysis were from eBioscience unless otherwise noted: anti-mouse CD11b eFluor® 450, anti-mouse F4/80 antigen PE-Cy7, antimouse CD4 eFluor® 450 and anti-mouse CD4 PE-Cy7 (BD

pharmingen). Flow cytometric analysis was performed on a BD LSRFortessa flow cytometer (BD Biosciences).

2.12. Statistical analysis

Statistical analysis was performed using ANOVA test followed by a Bonferroni post-hoc test (GraphPad Prism) or Student's *t*-test. Data were expressed as mean ± standard error of mean (S.E.M.). Statistical significance was represented by $*p < 0.05$ and $**p < 0.01$.

3. Results

3.1. Blockade of TNFα during colitis inhibits IL-22 production

Initially, we investigated whether blockade of TNFα using anti-TNFα antibody affected the production of IL-22 during colitis. As expected, TNFα expression level in the anti-TNFα antibody-treated mouse group was significantly lower than that in the PBS control group (Fig. 1). However, IL-22 expression level also remarkably decreased after the treatment of anti-TNFα antibody. Since IL-22 played an extremely important role in mucosal healing, we speculated that co-administration of TNFα inhibitor and IL-22 might facilitate the recovery of colitis with respect to anti-inflammation and mucosal healing. Therefore, we conducted the following investigations to verify this hypothesis.

3.2. Preparation of NPs

Gal-siRNA-NPs were produced using a water-in-oil-in-water (W/O/W) double emulsion-solvent evaporation method, which is a well-established technique for fabricating siRNA-loaded PLGA NPs [41]. The inner aqueous phase (containing siRNA/spermidine complexes) was mixed with the organic phase (containing PLGA) to form the first W/O emulsion under vortex and sonication. Thereafter, we added this first emulsion to the second aqueous phase (containing an emulsifier) and performed sonication to form a W/O/W emulsion based on the Gibbs-Marangoni effect and a capillary break-up mechanism [42]. With the evaporation of DCM, the inner aqueous phase (siRNA/spermidine complexes) was efficiently restricted into the hydrophobic PLGA matrix.

The emulsifiers at NP surface enabled the separation of oil phase and water phase, and thus prevented NPs from aggregation [43]. PVA is a common amphiphilic copolymer that has been extensively applied as an emulsifier for preparing PLGA polymeric NPs [44]. During the fabrication process of NPs, the hydrophobic parts of PVA penetrate into the organic phase and are entrapped in the polymeric matrix of NPs, while the hydrophilic parts form the NP corona and further stabilize the particle through steric hindrance. Chitosan is a natural biocompatible polymer, and it has been used for the surface modification of PLGA polymeric NPs in our group [45]. Its coating ability may reflect the entangling of its chains with PVA and/or the adsorption of positive-charged chitosan to the negative-charged surfaces of NPs. Finally, LA was conjugated to the CS-coated NPs *via* the formation of an ester bond between the carboxyl group of LA and the amino group of chitosan at the distal end of NPs. Based on this strategy, we successfully obtained the desired Gal-siRNA-loaded NPs (Fig. 2a), and its galactose content in Gal-siTNF-NPs was measured to be 0.23 mg/g Gal-siTNF-NPs using a modified anthrone sulfuric acid method.

3.3. Physicochemical characterizations of NPs

Particle size, polydispersity index (PDI) and zeta potential are important parameters that impact the stability, drug release behavior, cellular uptake profile and *in vivo* bio-distribution of NPs [46]. Thus, these parameters were characterized in an acidic solution (pH 6.2) resembling the physiological pH condition in colonic lumen. As presented in Table 1, dynamic light scattering (DLS) measurements revealed that the average hydrodynamic particle size of siTNF-NPs was 255.7 nm, and that of Gal-siTNF-NPs was 261.3 nm. Additionally, we found that these two types of NPs exhibited a slightly negative zeta potential of around −8.0 mV.

Fig. 2b,c showed the representative scanning electron microscopy (SEM) and transmission electron microscopy (TEM) images of siTNF-NPs (Fig. 2b) and Gal-siTNF-NPs (Fig. 2c). It was obvious that they had a spherical shape with smooth surface morphology, and most of the unhydrated NPs had diameters ranging from 85.8 nm to 157.3 nm. In addition, there was no detectable difference in the morphology or surface roughness between siTNF-NPs and Gal-siTNF-NPs. The discrepancy in the particle sizes measured by DLS and SEM/TEM may be due to the different NP surface states under dissimilar test conditions. As described in our previous study [47], NPs are in a fully swollen state when examined by DLS, whereas they are completely dehydrated for SEM/TEM characterization. As reported, cells are inclined to internalize NPs with particle sizes < 400 nm [48, 49]. On the other hand, NPs with particle sizes <10 μm preferentially accumulate in colitis tissues based on the epithelial enhanced permeability and retention (eEPR) effect, which is attributed to the disordered nature of the mucosal barrier, the impairment of epithelial tight junctions and the accumulation of immune cells. Moreover, large amount of positively charged glycoproteins are accumulated in the surface of inflamed mucosa [50]. Therefore, the particle size and zeta potential of our Gal-siTNF-NPs should favor their adhesion to the positive-charged inflamed mucosa, penetration into inflamed colon tissue and further internalization into target cells.

The *in vitro* siRNA release patterns of NPs were examined at pH 7.4 and pH 6.2, respectively. As seen in Fig. S1, Gal-siTNF-NPs exhibited a triphasic release behavior. Specifically, a slightly burst release of siRNA from Gal-siTNF-NPs was detected in the initial 4 h followed by a continuous release over a period of 44 h. Thereafter, the siRNA release was at a much lower but constant rate. Furthermore, it was found that the accumulative release percentages of siRNA from Gal-siTNF-NPs were 59.6% and 74.9% at pH 7.4 and pH 6.2, respectively. The reason for the increase in siRNA release percentage at pH 6.2 might be that the PLGA polymeric matrix of Gal-siTNF-NPs degrades more rapidly under acidic condition than that in a neutral environment.

Subsequently, electrophoresis was utilized to confirm the integrity of siRNA, which was extracted from NPs. As shown in Fig. S2a, in comparison with control siRNA (Lane 1), siRNA extracted from NPs appeared intact (Lane 2), suggesting that siRNA fragments kept its integrity during the fabrication, freeze-drying and extraction process. It was noting that the band in Fig. S2a corresponding to siRNA fragments from Gal-siTNF-NPs (Lane 2) was slightly lagging behind the control siRNA (Lane 1). This can be ascribed to the fact that electro-osmosis occurs in agarose gel upon the action of electric field. With regard to siRNA from NPs, they were mixed with the constituents of Tris-EDTA (TE) buffer (10 mM Tris-

HCl, 1 mM EDTA, pH = 8.0) after lyophilization, and the concentrated ions play an important part in the movement of siRNA in electric field. Meanwhile, we also found that bromophenol blue and xylene cyanol FF from the Loading Dye in Lane 2 were slightly lagging behind that in Lane 1 during electrophoresis (Fig. S2b).

3.4. Biocompatibility tests of NPs

To evaluate the biocompatibility properties of the developed NPs, we performed *in vitro* cytotoxicity tests against Raw 264.7 macrophages and Colon-26 cells. The results from MTT assays (Fig. 3a–d) revealed that there was no obvious cytotoxicity in either cell line following incubation with siTNF-NPs or Gal-siTNF-NPs, even after 48 h. OF is a commercial siRNA transfection reagent and has been widely used as a gold standard for evaluating the transfection efficiency of siRNA delivery systems. Accordingly, it was used as another control in the present study. After 48 h of incubation, OF/siTNF complexes inhibited the cell viability of Raw 264.7 macrophages and Colon-26 cells by over 35.4% and 33.1%, respectively. These results collectively indicate that siTNF-NPs and Gal-siTNF-NPs have excellent biocompatibility.

3.5. Cellular uptake profiles of NPs

Since siTNF exerts its function in the cytoplasm [51], efficient cellular uptake is a major requirement for the therapeutic efficacy of siRNA-loaded NPs. To track the Gal-functionalized NPs in cells, we used FITC-siRNA as a fluorescent probe. As can be seen in Fig. 4a, untreated control cells showed no fluorescence, whereas clear green fluorescence was observed in the cells with the treatment of Gal-FITC-siRNA-NPs (FITC-siRNA, 100 ng/mL) or OF/FITC-siRNA complexes. Moreover, Gal-FITC-siRNA-NPs yielded comparable FITC fluorescence intensities to OF/FITC-siRNA complexes. We also found that Gal-FITC-siRNA-NPs were internalized into cytoplasm, not the nucleus. This is consistent to the general recognition that nuclear pore complexes are typically between 20 and 50 nm, which limit the access of NPs with diameters > 200 nm. In addition, we also found that the nucleus of cells treated with OF/FITC-siRNA complexes showed deformation and chromatin condensation, which might be due to their strong cytotoxicity (Fig. 3).

To quantitatively compare the cellular uptake efficiencies of non-functionalized NPs and Gal-functionalized NPs, we treated Raw 264.7 macrophages with FITC-siRNA-NPs or Gal-FITC-siRNA-NPs, and further investigate their cellular uptake profiles after 0, 1, 3 and 5h of co-incubation. Fig. 4c indicated that the fluorescence intensities were dramatically higher in the Gal-FITC-siRNA-NP-treated Raw 264.7 macrophages compared with the corresponding FITC-siRNA-NP-treated cells. This implies that the surface functionalization with galactose can endow NPs with the property of targeted siRNA delivery to the target cells (Raw 264.7 macrophages).

3.6. In vitro anti-inflammatory activities of NPs

We treated Raw 264.7 macrophages with NPs, and further examined their mRNA expression levels of TNFα, which was highly secreted by macrophages during the onset and progression of UC [52]. Fig. 5 implied that macrophages treated with LPS (1 μg/mL; to stimulate an inflammatory response) exhibited remarkable increase in TNFα mRNA

expression level. However, this effect was considerably reduced in cells pre-treated with siTNF-loaded NPs. Furthermore, we found that cells treated with Gal-siTNF-NPs showed significantly lower TNFα mRNA expression levels than those treated with siTNF-NPs. LPS-treated macrophages which were pre-treated with Gal-siTNF-NPs maintained their decreased levels of TNFα even after 72 h and 96 h of treatment (Fig. S3). In combination with the data of *in vitro* cellular uptake studies (Fig. 4b,c), these results suggest that LA functionalization is liable to enhance the cellular uptake of NPs through galactose receptor-mediated endocytosis, and further improve the TNFα gene silencing. Notably, the Gal-siTNF-NP-mediated decrease in TNFα expression did not significantly differ from that induced by the leading commercial product (OF/siTNF complexes), indicating that Gal-siTNF-NPs could exert an efficient anti-inflammatory effect on LPS-treated macrophages.

3.7. Promotion of mucosal healing by IL-22

Enhancement of mucosal healing is one of the two major therapeutic goals in UC treatment [53]. Here, we investigated the impact of IL-22 on wound healing using ECIS. Caco2-BBE monolayers grown on ECIS 8W1E plates were wounded with a 30-s electrical pulse (frequency, 40 kHz; amplitude, 4.5 V). As shown in Fig. 6, wounded epithelial layers treated with IL-22 showed significant and dose-dependent increase in recovery, in comparison with untreated control layers. These results clearly demonstrate that IL-22 can enhance the healing of a wounded colonic epithelial layer.

3.8. In vivo distribution profiles of drug formulations

The DSS-induced UC mouse model is an easily generated and highly reproducible model that resembles human UC (*e.g.*, body weight loss, colonic ulcers and bloody stool), and thus it has been extensively used to evaluate the new drug formulations for UC treatment [54–56]. DSS is given in drinking water and can disrupt the epithelial integrity of colon; inflammation and colitis can be seen within 1 week after treatment. To investigate the *in vivo* bio-distribution of Gal-functionalized NPs in GIT, we gavaged Gal-DiR-NP-embedded hydrogel in mice with UC, and examined the time-dependent passage and *in vivo* targeting efficacy of this drug formulation using near infrared fluorescence (NIRF) imaging.

Initially, to confirm the uniform distribution of NPs in hydrogel, NP-embedded hydrogel was freeze-dried, cut transversely and observed under SEM. Fig. S4a,b indicated that hydrogel matrix in the absence of NPs showed a pretty smooth surface. In contrast, hydrogel matrix with NPs exhibited a rough surface (Fig. S4c,d). Moreover, we found that NPs were homogenously dispersed within the hydrogel matrix, which would protect drugs during their passage through GIT and specifically release them in colonic lumen or even targeted cells. Accordingly, we further investigated the release behaviors of drugs (siTNF and IL-22) from Gal-siTNF-NP/IL-22-embedded hydrogel. It was found that no siRNA was detected in the releasing buffer (data not shown). In the context of protein embedded in hydrogel (Fig. S5), its release rate was much slower in the presence of simulated gastric fluid (pH 1.2) and simulated intestinal fluid (pH 7.4) than that in simulated colonic fluid (pH 6.8), suggesting that hydrogel would collapse in the colon environment. As reported, the lengths of detention time for oral administered matters were normally 2 h and 4 h in stomach and small intestine, respectively [36, 57]. Thus, only a small amount (< 14.4%) of protein was released from

hydrogel during their passage through upper GIT, whereas most protein drug (over 59.6%) was released into colonic lumen within 12 h. These results clearly demonstrated that hydrogel could efficiently protect the loaded drugs in the upper intestine and specifically release them in colonic lumen.

As presented in Fig. 7a,b, a strong NIRF signal was detected in colon and small intestine after 4 h of oral administration. With the passage of time, the NIRF signal gradually decreased, indicating that the rapid clearance of NPs occurred in the feces. It was obvious that little to no fluorescence was observed in colon by 24 h post-administration, and mice were thus gavaged daily for treatments.

To attempt to investigate the bio-distribution profiles of Gal-functionalized NPs in healthy colon tissue or inflamed colon tissue, we orally administered mice with Gal-FITC-siRNA-NP-embedded hydrogel. Once the NPs were released from hydrogel, they had to go through the mucus layer and be internalized by target cells. As can be seen in Fig. 7c, tissue cross sections revealed that only a handful of the colonic epithelial cells in healthy colon tissue internalized NPs (green) by 12 h after oral administration of Gal-FITC-siRNA-NPs. Conversely, a number of colonic cells in colitis tissues showed green fluorescence. These results clearly indicate that Gal-FITC-siRNA-NPs have the capacity to penetrate deeply into the mucosa *via* the eEPR effect and were taken up by the target cells (*e.g.*, macrophages).

To further quantify the percentage of macrophages in colitis tissue that internalized Gal-functionalized NPs, we gavaged DSS-treated mice with FITC-siRNA-NP- or Gal-FITC-siRNA-embedded hydrogel, and further carried out FCM analysis. Macrophages have traditionally been considered to be part of a linear mononuclear phagocytic system, and are believed to be exclusively derived from blood monocytes [58]. It has been reported previously that monocytes can give rise to intestinal macrophages during inflammation in both humans and mice [59, 60]. However, more recent research suggested that macrophages might derive from two sources: embryonic precursors (characterized as CD11b + F4/80^{hi} cells) and conventional hematopoiesis (characterized as CD11b + F4/80^{lo} cells) [61]. Fig. S6 shows the analytic processes that we used to examine macrophages arising from both sources. As shown in Fig. 7d, 78.1% and 8.5% of CD11b + F4/80^{lo} colonic macrophages and CD11b + F4/80^{hi} macrophages, respectively, had taken up Gal-FITC-siRNA-NPs by 12 h of post-administration, whereas these percentages were only 63.4% and 4.5%, respectively, in FITC-siRNA-NP-treated mice. These results confirm the targeting capability of the surface-conjugated galactose groups *in vivo*, which are consistent with our *in vitro* results (Fig. 4c).

3.9. In vivo therapeutic efficacy of drug formulations against UC

We next investigated whether oral administration of hydrogel-encapsulated Gal-siTNF-NPs and IL-22 could exert synergistic therapeutic effects against DSS-induced UC in mice. Body weight loss is typically used as a main marker of the colitis phenotype in this model. Thus, we examined the changes of body weight among DSS-induced mouse groups treated with hydrogel loaded with Gal-siTNF-NPs and/or IL-22. As presented in Fig. 8a, DSS-treated control mice exhibited a body weight loss that peaked on day 14. However, the Gal-siTNF-

NP/IL-22-treated group showed the smallest body weight loss among the groups on days 12 and 13, and showed the best body weight recovery among these four DSS-treated groups.

MPO activity is a direct indicator of the infiltration of neutrophils into the colonic mucosa, and is thus an important marker of inflammation during DSS treatment. Fig. 8b indicated that the colonic MPO activities were significantly lower in the three Gal-siTNF-NP- and/or IL-22-treated groups than in the DSS-treated control group. The DSS-treated control group has a significantly higher spleen weight compared to the healthy control group. The spleen weights of the three Gal-siTNF-NP- and/or IL-22-treated groups did not differ significantly from that in the healthy control group (Fig. 8c). Moreover, Gal-siTNF-NP- or IL-22-treated mice showed significantly shorter colon lengths compared to the healthy control group, whereas the colon length of Gal-siTNF-NP/IL-22-treated group did not significantly differ from that of the healthy control group (Fig. 8d). In terms of mRNA expression levels, we observed remarkable increases of colonic TNFα expression in the DSS-treated control group, Gal-siTNF-NP-treated group and IL-22-treated group; however, there was no marked difference in this parameter between the Gal-siTNF-NP/IL-22-treated group and the healthy control group (Fig. 8e).

Hematoxylin and eosin (H&E)-stained colon cryosections were evaluated for histological changes. Colon tissues from the healthy control group were characterized by normal colon histology, with no sign of inflammation or disruption of healthy tissue morphology (Fig. 9a). In contrast, colon tissues from the DSS-treated control group exhibited clear signs of inflammation, including epithelial disruption, goblet cell depletion and significant infiltration of inflammatory cells into the mucosa (Fig. 9b). Tissues from the treatment groups showed much less inflammation (Fig. 9c-e). Indeed, colon tissues from the Gal-siTNF-NP/IL-22-treated group exhibited almost the same tissue morphology as that observed in the healthy control group, especially with respect to the integration of the colonic epithelial layer and the infiltration of inflammatory cells (Fig. 9e). The histological score of the DSS-treated control group was significantly higher than those of the other four mouse groups (Fig. 9f). In addition, the Gal-siTNF-NP/IL-22-treated group showed the lowest histological score among the three treatment groups. In summary, our results clearly demonstrate that combined treatment with Gal-siTNF-NPs plus IL-22 yields the highest therapeutic efficacy among three tested groups, and could efficiently promote the recovery of colon tissue from UC, as summarized in our schematic illustration.

4. Conclusions

We herein report the first example of targeted co-delivery of TNFα siRNA (siTNF) and IL-22 *via* an orally administered NP-in-hydrogel system for the treatment of ulcerative colitis (UC). We conclude the following concerning the synergistic therapeutic effect of this combined therapeutic: (1) Gal-functionalized NPs can realize targeted delivery of siTNF to macrophages and produce much better anti-inflammatory activity compared with non-functionalized NPs; (2) IL-22 can efficiently achieve mucosal healing; (3) Orally administered Gal-siTNF-NP/IL-22-embedded hydrogel exhibits a much better therapeutic effect against UC compared with the corresponding single drug-based formulations. We

believe that this effective and biocompatible formulation offers a promising approach for the synergistic combined treatment of UC.

Supplementary Material

Refer to Web version on PubMed Central for supplementary material.

Acknowledgements

This work was supported by the National Institutes of Health of Diabetes and Digestive and Kidney (RO1DK116306, RO1DK107739 and RO1DK071594), the Litwin IBD Pioneers initiative, the National Natural Science Foundation of China (51503172 and 81571807), the Department of Veterans Affairs (Merit Award BX002516 to D.M.), the Fundamental Research Funds for the Central Universities (XDJK2017B058), the Young Core Teacher Program of the Municipal Higher Educational Institution of Chongqing and the State Key Laboratory of Silkworm Genome Biology. D.M. is a recipient of a Senior Research Career Scientist Award from the Department of Veterans Affairs.

References

[1]. Peterson LW, Artis D, Intestinal epithelial cells: regulators of barrier function and immune homeostasis, Nat. Rev. Immunol 14 (2014) 141–153. [PubMed: 24566914]

[2]. Luissint AC, Parkos CA, Nusrat A, Inflammation and the intestinal barrier: leukocyte-epithelial cell interactions cell junction remodeling, and mucosal repair, Gastroenterology 151 (2016) 616–632. [PubMed: 27436072]

[3]. da Silva BC, Lyra AC, Rocha R, Santana GO, Epidemiology, demographic characteristics and prognostic predictors of ulcerative colitis, World J. Gastroenterol 20 (2014) 9458–9467. [PubMed: 25071340]

[4]. Gionchetti P, Rizzello F, Annese V, Armuzzi A, Biancone L, Castiglione F, Comberlato M, Cottone M, Danese S, Daperno M, D'Inca R, Fries W, Kohn A, Orlando A, Papi C, Vecchi M, Ardizzone S, Bo IGSI, Use of corticosteroids and immunosuppressive drugs in inflammatory bowel disease: clinical practice guidelines of the Italian Group for the Study of inflammatory bowel disease, Dig. Liver Dis 49 (2017) 604–617. [PubMed: 28254463]

[5]. Barnes EL, Nestor M, Onyewadume L, de Silva PS, Korzenik JR, Investigators D, High dietary intake of specific fatty acids increases risk of flares in patients with ulcerative colitis in remission during treatment with aminosalicylates, Clin. Gastroenterol. Hepatol 15 (2017) 1390–1396. [PubMed: 28110099]

[6]. Sandborn WJ, Strategies for targeting tumour necrosis factor in IBD, Best Pract. Res. Cl. Ga 17 (2003) 105–117.

[7]. Papa A, Mocci G, Bonizzi M, Felice C, Andrisani G, Papa G, Gasbarrini A, Biological therapies for inflammatory bowel disease: controversies and future options, Expert. Rev. Clin. Pharmacol 2 (2009) 391–403. [PubMed: 22112183]

[8]. Etzerodt A, Maniecki MB, Graversen JH, Moller HJ, Torchilin VP, Moestrup SK, Efficient intracellular drug-targeting of macrophages using stealth liposomes directed to the hemoglobin scavenger receptor CD163, J. Control. Release 160 (2012) 72–80. [PubMed: 22306335]

[9]. Song Y, Kim YR, Kim SM, Ain QU, Jang K, Yang CS, Kim YH, RNAi-mediated silencing of TNF-alpha converting enzyme to down-regulate soluble TNF-alpha production for treatment of acute and chronic colitis, J. Control. Release 239 (2016) 231–241. [PubMed: 27562600]

[10]. Hoentjen F, Van Bodegraven AA, Safety of anti-tumor necrosis factor therapy in inflammatory bowel disease, World J. Gastroenterol 15 (2009) 2067–2073. [PubMed: 19418577]

[11]. Aouadi M, Tesz GJ, Nicoloro SM, Wang E, Chouinard M, Soto E, Ostroff GR, Czech MP, Orally delivered siRNA targeting macrophage Map4k4 suppresses systemic inflammation, Nature 458 (2009) 1180–1184. [PubMed: 19407801]

[12]. Laroui H, Viennois E, Xiao B, Canup BS, Geem D, Denning TL, Merlin D, Fab'-bearing siRNA TNFalpha-loaded nanoparticles targeted to colonic macrophages offer an effective therapy for experimental colitis, J. Control. Release 186 (2014) 41–53. [PubMed: 24810114]

[13]. Yin LC, Song ZY, Qu QH, Kim KH, Zheng N, Yao C, Chaudhury I, Tang HY, Gabrielson NP, Uckun FM, Cheng JJ, Supramolecular self-assembled nanoparticles mediate oral delivery of therapeutic TNF-alpha siRNA against systemic inflammation, Angew. Chem. Int. Ed 52 (2013) 5757–5761.

[14]. Oe Y, Christie RJ, Naito M, Low SA, Fukushima S, Toh K, Miura Y, Matsumoto Y, Nishiyama N, Miyata K, Kataoka K, Actively-targeted polyion complex micelles stabilized by cholesterol and disulfide cross-linking for systemic delivery of siRNA to solid tumors, Biomaterials 35 (2014) 7887–7895. [PubMed: 24930854]

[15]. Buyens K, De Smedt SC, Braeckmans K, Demeester J, Peeters L, van Grunsven LA, de X du Jeu Mollerat, Sawant R, Torchilin V, Farkasova K, Ogris M, Sanders NN, Liposome based systems for systemic siRNA delivery: stability in blood sets the requirements for optimal carrier design, J. Control. Release 158 (2012) 362–370. [PubMed: 22023849]

[16]. Xiao B, Xu Z, Viennois E, Zhang Y, Zhang Z, Zhang M, Han MK, Kang Y, Merlin D, Orally targeted delivery of tripeptide KPV via hyaluronic scid-functionalized nanoparticles efficiently alleviates ulcerative colitis, Mol. Ther 25 (2017) 1628–1640. [PubMed: 28143741]

[17]. Si XY, Merlin D, Xiao B, Recent advances in orally administered cell-specific nanotherapeutics for inflammatory bowel disease, World J. Gastroenterol 22 (2016) 7718–7726. [PubMed: 27678353]

[18]. Sakakura M, Oo-Puthinan S, Moriyama C, Kimura T, Moriya J, Irimura T, Shimada I, Carbohydrate binding mechanism of the macrophage galactose-type C-type lectin 1 revealed by saturation transfer experiments, J. Biol. Chem 283 (2008) 33665–33673. [PubMed: 18790731]

[19]. Wang HW, Jiang PL, Lin SF, Lin HJ, Ou KL, Deng WP, Lee LW, Huang YY, Liang PH, Liu DZ, Application of galactose-modified liposomes as a potent antigen presenting cell targeted carrier for intranasal immunization, Acta Biomater. 9 (2013) 5681–5688. [PubMed: 23159567]

[20]. Zhang J, Tang C, Yin CH, Galactosylated trimethyl chitosan-cysteine nanoparticles loaded with Map4k4 siRNA for targeting activated macrophages, Biomaterials 34 (2013) 3667–3677. [PubMed: 23419643]

[21]. Wu F, Wuensch SA, Azadniv M, Ebrahimkhani MR, Crispe IN, Galactosylated LDL nanoparticles: a novel targeting delivery system to deliver antigen to macrophages and enhance antigen specific T cell responses, Mol. Pharm 6 (2009) 1506–1517. [PubMed: 19637876]

[22]. Chavez-Santoscoy AV, Roychoudhury R, Pohl NLB, Wannemuehler MJ, Narasimhan B, Ramer-Tait AE, Tailoring the immune response by targeting C-type lectin receptors on alveolar macrophages using "pathogen-like" amphiphilic polyanhydride nanoparticles, Biomaterials 33 (2012) 4762–4772. [PubMed: 22465338]

[23]. de Chambrun GP, Peyrin-Biroulet L, Lemann M, Colombel JF, Clinical implications of mucosal healing for the management of IBD, Nat. Rev. Gastroenterol. Hepatol 7 (2010) 15–29. [PubMed: 19949430]

[24]. Iacucci M, de Silva S, Ghosh S, Mesalazine in inflammatory bowel disease: a trendy topic once again? Can. J. Gastroenterol 24 (2010) 127–133. [PubMed: 20151072]

[25]. Ni M, Chen C, Qian J, Xiao HX, Shi WF, Luo Y, Wang HY, Li Z, Wu J, Xu PS, Chen SH, Wong G, Bi YH, Xia ZP, Li W, Lu HJ, Ma JC, Tong YG, Zeng H, Wang SQ, Gao GF, Bo XC, Liu D, Intra-host dynamics of ebola virus during 2014, Nat. Microbiol 1 (2016) 16151. [PubMed: 27595345]

[26]. Lee YY, Gangireddy V, Khurana S, Rao SSC, Are we ready for combination therapy in moderate-to-severe ulcerative colitis? Gastroenterology 147 (2014) 544.

[27]. Zindl CL, Lai JF, Lee YK, Maynard CL, Harbour SN, Ouyang W, Chaplin DD, Weaver CT, IL-22-producing neutrophils contribute to antimicrobial defense and restitution of colonic epithelial integrity during colitis, P. Natl. Acad. Sci. USA 110 (2013) 12768–12773.

[28]. Ouyang WJ, Distinct roles of IL-22 in human psoriasis and inflammatory bowel disease, Cytokine Growth Factor Rev. 21 (2010) 435–441. [PubMed: 21106435]

[29]. Sugimoto K, Ogawa A, Mizoguchi E, Shimomura Y, Andoh A, Bhan AK, Blumberg RS, Xavier RJ, Mizoguchi A, IL-22 ameliorates intestinal inflammation in a mouse model of ulcerative colitis, J. Clin. Invest 118 (2008) 534–544. [PubMed: 18172556]

[30]. Zenewicz LA, Yancopoulos GD, Valenzuela DM, Murphy AJ, Stevens S, Flavell RA, Innate and adaptive interleukin-22 protects mice from inflammatory bowel disease, Immunity 29 (2008) 947–957. [PubMed: 19100701]

[31]. Neufert C, Pickert G, Zheng Y, Wittkopf N, Warntjen M, Nikolaev A, Ouyang WJ, Neurath MF, Becker C, Activation of epithelial STAT3 regulates intestinal homeostasis, Cell Cycle 9 (2010) 652–655. [PubMed: 20160497]

[32]. Pickert G, Neufert C, Leppkes M, Zheng Y, Wittkopf N, Warntjen M, Lehr HA, Hirth S, Weigmann B, Wirtz S, Ouyang W, Neurath MF, Becker C, STAT3 links IL-22 signaling in intestinal epithelial cells to mucosal wound healing, J. Exp. Med 206 (2009) 1465–1472. [PubMed: 19564350]

[33]. Danhier F, Ansorena E, Silva JM, Coco R, Le Breton A, Preat V, PLGA-based nanoparticles: an overview of biomedical applications, J. Control. Release 161 (2012) 505–522. [PubMed: 22353619]

[34]. Jensen DK, Jensen LB, Koocheki S, Bengtson L, Cun D, Nielsen HM, Foged C, Design of an inhalable dry powder formulation of DOTAP-modified PLGA nanoparticles loaded with siRNA, J. Control. Release 157 (2012) 141–148. [PubMed: 21864597]

[35]. Xiao B, Zhang Z, Viennois E, Kang Y, Zhang M, Han MK, Chen J, Merlin D, Combination therapy for ulcerative colitis: orally targeted nanoparticles prevent mucosal damage and relieve inflammation, Theranostics 6 (2016) 2250–2266. [PubMed: 27924161]

[36]. Xiao B, Viennois E, Chen Q, Wang L, Han MK, Zhang Y, Zhang Z, Kang Y, Wan Y, Merlin D, Silencing of intestinal glycoprotein CD98 by orally targeted nanoparticles enhances chemosensitization of colon cancer, ACS Nano 12 (2018) 5253–5265. [PubMed: 29860836]

[37]. Xiao B, Laroui H, Viennois E, Ayyadurai S, Charania MA, Zhang Y, Zhang Z, Baker MT, Zhang B, Gewirtz AT, Merlin D, Nanoparticles with surface antibody against CD98 and carrying CD98 small interfering RNA reduce colitis in mice, Gastroenterology 146 (2014) 1289–1300. [PubMed: 24503126]

[38]. Laroui H, Geem D, Xiao B, Viennois E, Rakhya P, Denning T, Merlin D, Targeting intestinal inflammation with CD98 siRNA/PEI-loaded nanoparticles, Mol. Ther 22 (2014) 69–80. [PubMed: 24025751]

[39]. Denning TL, Wang YC, Patel SR, Williams IR, Pulendran B, Lamina propria macrophages and dendritic cells differentially induce regulatory and interleukin 17-producing T cell responses, Nat. Immunol 8 (2007) 1086–1094. [PubMed: 17873879]

[40]. Denning TL, Norris BA, Medina-Contreras O, Manicassamy S, Geem D, Madan R, Karp CL, Pulendran B, Functional specializations of intestinal dendritic cell and macrophage subsets that control Th17 and regulatory T cell responses are dependent on the T cell/APC ratio, source of mouse strain, and regional localization, J. Immunol 187 (2011) 733–747. [PubMed: 21666057]

[41]. Cohen-Sela E, Chorny M, Koroukhov N, Danenberg HD, Golomb G, A new double emulsion solvent diffusion technique for encapsulating hydrophilic molecules in PLGA nanoparticles, J. Control. Release 133 (2009) 90–95. [PubMed: 18848962]

[42]. Mora-Huertas CE, Fessi H, Elaissari A, Influence of process and formulation parameters on the formation of submicron particles by solvent displacement and emulsification-diffusion methods critical comparison, Adv. Colloid Interfac 163 (2011) 90–122.

[43]. Mu L, Feng SS, PLGA/TPGS nanoparticles for controlled release of paclitaxel: effects of the emulsifier and drug loading ratio, Pharm. Res 20 (2003) 1864–1872. [PubMed: 14661934]

[44]. Hassan CM, Peppas NA, Structure and applications of poly(vinyl alcohol) hydrogels produced by conventional crosslinking or by freezing/thawing methods, Adv. Polym. Sci 153 (2000) 37–65.

[45]. Xiao B, Han MK, Viennois E, Wang L, Zhang M, Si X, Merlin D, Hyaluronic acid-functionalized polymeric nanoparticles for colon cancer-targeted combination chemotherapy, Nanoscale 7 (2015) 17745–17755. [PubMed: 26455329]

[46]. He C, Hu Y, Yin L, Tang C, Yin C, Effects of particle size and surface charge on cellular uptake and biodistribution of polymeric nanoparticles, Biomaterials 31 (2010) 3657–3666. [PubMed: 20138662]

[47]. Xiao B, Cui LQ, Chen TM, Lian B, Stochastic effects in adaptive reconstruction of body damage: implied the creativity of natural selection, J. Cell. Mol. Med 19 (2015) 2521–2529. [PubMed: 26153081]

[48]. Kim TH, Ihm JE, Choi YJ, Nah JW, Cho CS, Efficient gene delivery by urocanic acid-modified chitosan, J. Control. Release 93 (2003) 389–402. [PubMed: 14644588]

[49]. Liu Y, Reineke TM, Hydroxyl stereochemistry and amine number within poly (glycoamidoamine)s affect intracellular DNA delivery, J. Am. Chem. Soc 127 (2005) 3004–3015. [PubMed: 15740138]

[50]. Zhang S, Ermann J, Succi MD, Zhou A, Hamilton MJ, Cao B, Korzenik JR, Glickman JN, Vemula PK, Glimcher LH, Traverso G, Langer R, Karp JM, An inflammation-targeting hydrogel for local drug delivery in inflammatory bowel disease, Sci. Transl. Med 7 (2015) (300ra128).

[51]. Dalmasso G, Charrier-Hisamuddin L, Nguyen HT, Yan Y, Sitaraman S, Merlin D, PepT1-mediated tripeptide KPV uptake reduces intestinal inflammation, Gastroenterology 134 (2008) 166–178. [PubMed: 18061177]

[52]. Xiao B, Laroui H, Ayyadurai S, Viennois E, Charania MA, Zhang Y, Merlin D, Mannosylated bioreducible nanoparticle-mediated macrophage-specific TNF-alpha RNA interference for IBD therapy, Biomaterials 34 (2013) 7471–7482. [PubMed: 23820013]

[53]. Xiao B, Merlin D, Oral colon-specific therapeutic approaches toward treatment of inflammatory bowel disease, Expert Opin. Drug Del 9 (2012) 1393–1407.

[54]. Perse M, Cerar A, Dextran sodium sulphate colitis mouse model: traps and tricks, J Biomed Biotechnol 2012 (2012) 718617. [PubMed: 22665990]

[55]. Grisham MB, Do different animal models of IBD serve different purposes? Inflamm. Bowel Dis 14 (Suppl. 2) (2008) S132–S133. [PubMed: 18816751]

[56]. Wilson DS, Dalmasso G, Wang L, Sitaraman SV, Merlin D, Murthy N, Orally delivered thioketal nanoparticles loaded with TNF-alpha-siRNA target inflammation and inhibit gene expression in the intestines, Nat. Mater 9 (2010) 923–928. [PubMed: 20935658]

[57]. Xiao B, Si X, Zhang M, Merlin D, Oral administration of pH-sensitive curcumin-loaded microparticles for ulcerative colitis therapy, Colloid. Surf. B 135 (2015) 379–385.

[58]. van Furth R, Cohn ZA, Hirsch JG, Humphrey JH, Spector WG, Langevoort HL, The mononuclear phagocyte system: a new classification of macrophages, monocytes, and their precursor cells, B. World Health Organ 46 (1972) 845–852.

[59]. Grimm MC, Pullman WE, Bennett GM, Sullivan PJ, Pavli P, Doe WF, Direct evidence of monocyte recruitment to inflammatory bowel disease mucosa, J. Gastroenterol. Hepatol 10 (1995) 387–395. [PubMed: 8527703]

[60]. Platt AM, Bain CC, Bordon Y, Sester DP, Mowat AM, An independent subset of TLR expressing CCR2-dependent macrophages promotes colonic inflammation, J. Immunol 184 (2010) 6843–6854. [PubMed: 20483766]

[61]. Bain CC, Bravo-Blas A, Scott CL, Gomez Perdiguero E, Geissmann F, Henri S, Malissen B, Osborne LC, Artis D, Mowat AM, Constant replenishment from circulating monocytes maintains the macrophage pool in the intestine of adult mice, Nat. Immunol 15 (2014) 929–937. [PubMed: 25151491]

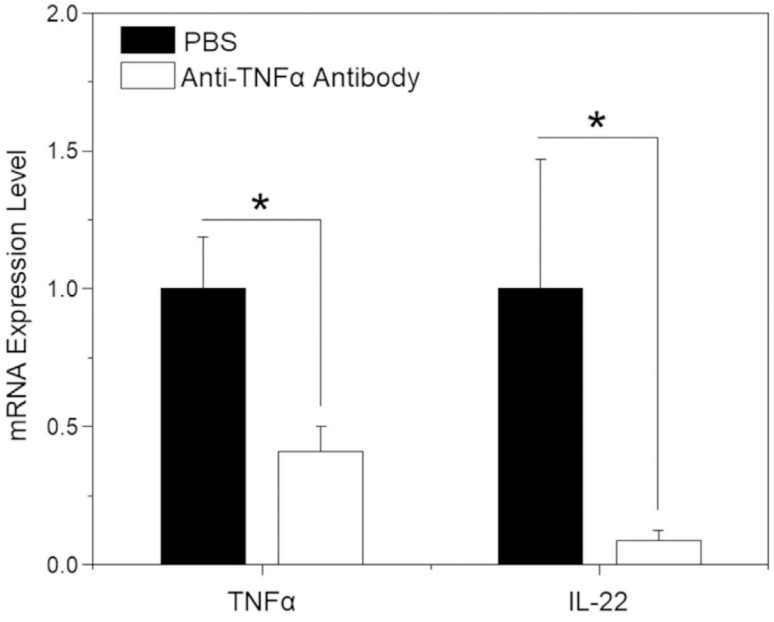

Fig. 1.

mRNA expression levels of TNFα and IL-22 in different mouse groups. IL10$^{-/-}$ mice were treated twice a week by intraperitoneal injection of PBS or anti-TNFα antibody solution from 4 to 14 weeks of age. Total RNA was extracted from colon tissues and the mRNA expression levels of TNFα and IL-22 were analyzed by RT-PCR. Each point represents the mean ± S.E.M. ($n = 7$; *$p < 0.05$, **$p < 0.01$).

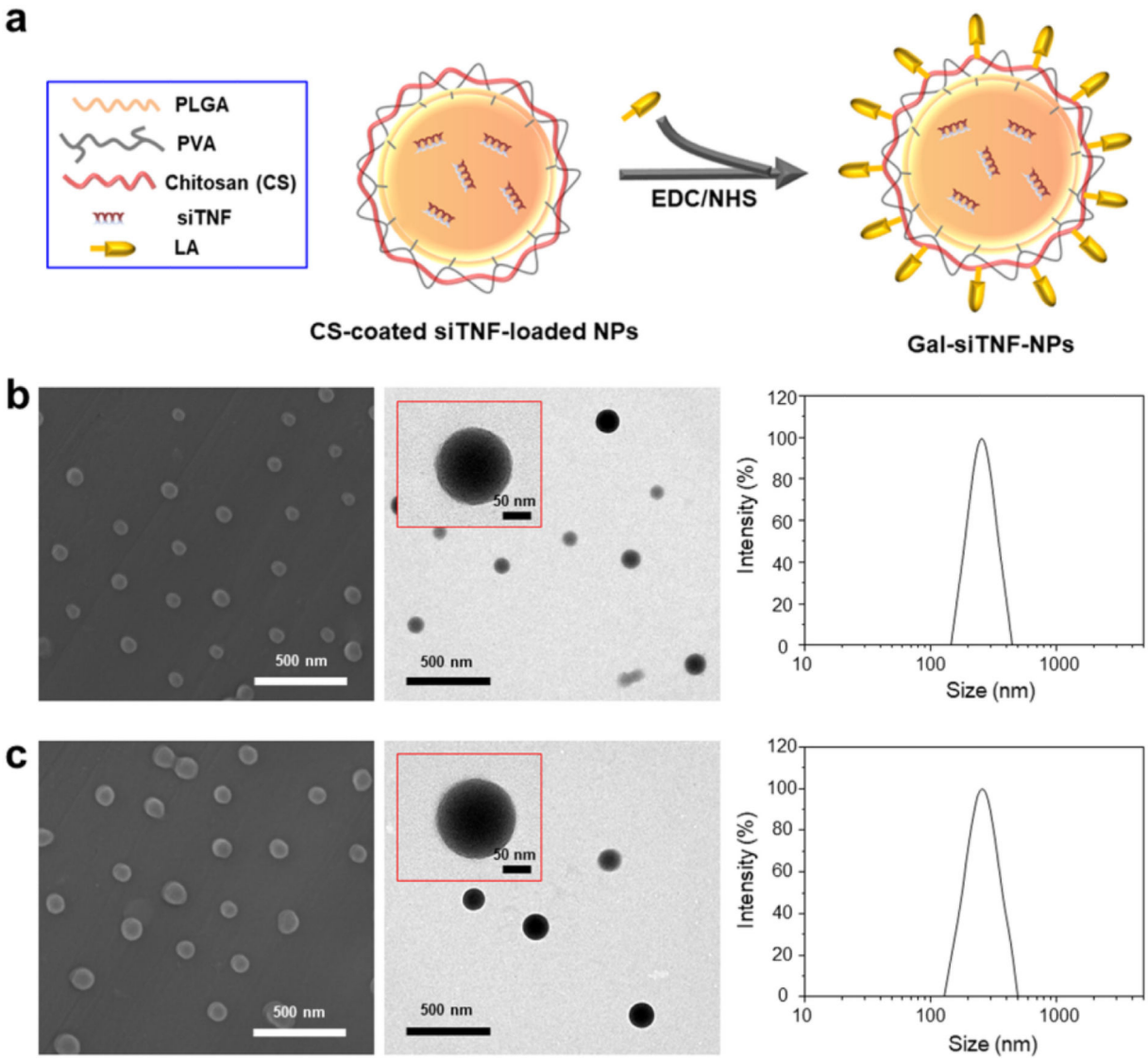

Fig. 2.

(a) Schematic illustration of the preparation of Gal-siTNF-NPs. Representative SEM, TEM and size distribution profiles of (b) siTNF-NPs and (c) Gal-siTNF-NPs.

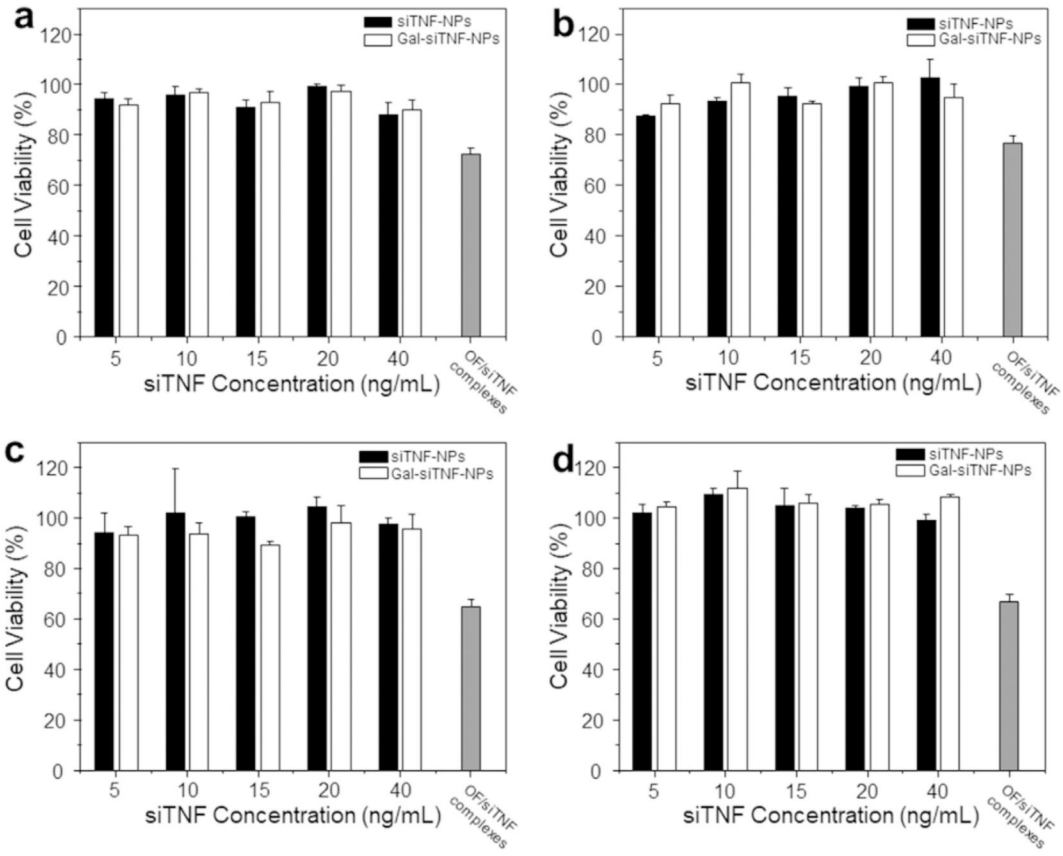

Fig. 3.

In vitro biocompatibility tests of siTNF-NPs and Gal-siTNF-NPs at different siTNF concentrations against Raw 264.7 macrophages and colon-26 cells. (a) Raw 264.7 macrophages for 24 h, (b) Colon-26 cells for 24 h, (c) Raw 264.7 macrophages for 48 h and (d) Colon-26 cells for 48 h. Triton X-100 was used as the positive control to produce a maximum cell death rate (100%). Cell culture medium was used as a negative control (death rate defined as 0%). OF/siTNF complexes were generated according to the manufacturer's standard protocols. Toxicity is given as the percentage of viable cells remaining after treatment. Each point represents the mean ± S.E.M. ($n = 5$).

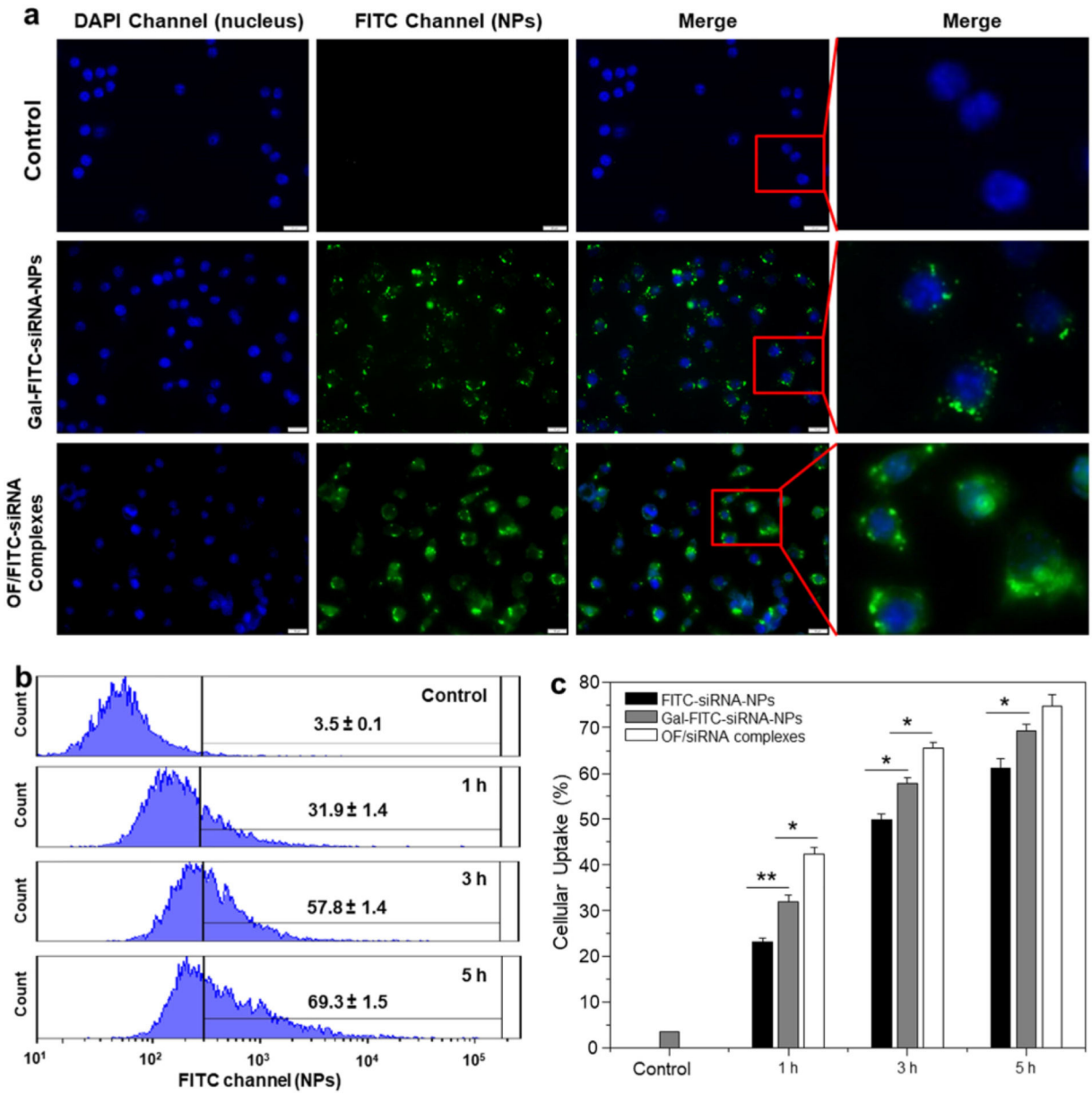

Fig. 4.

Cellular uptake profiles of NPs. (a) Images of cellular uptake of Gal-FITC-siRNA-NPs in Raw 264.7 macrophages at different time points (0, 3 and 5h). Cells were treated with Gal-FITC-siRNA-NPs (green), fixed and stained with DAPI (purple). Scale bar represents 10 μm. (b) Representative flow cytometric histograms of fluorescence intensities for cells treated with Gal-FITC-siRNA-NPs in Raw 264.7 macrophages at different time points (0, 1, 3 and 5h). (c) Percentage of FITC fluorescence-positive cells after treatments with FITC-siRNA-NPs, Gal-FITC-siRNA-NPs or OF/FITC-siRNA complexes for different time points (0, 1, 3 and 5 h). Each point represents the mean ± S.E.M. ($n = 3$; *$p < 0.05$, **$p < 0.01$, Student's t-test). (For interpretation of the references to colour in this figure legend, the reader is referred to the web version of this article.)

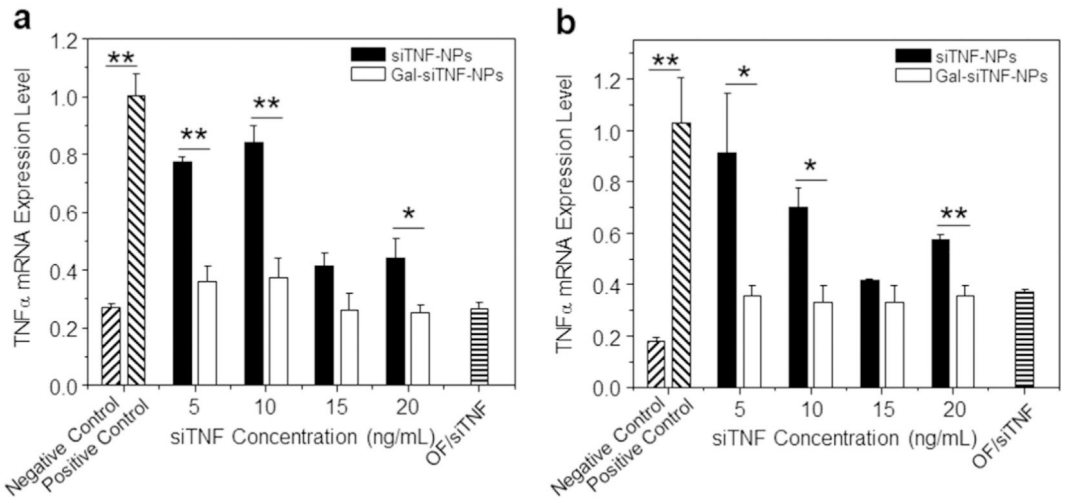

Fig. 5.

In vitro anti-inflammatory activities of siTNF-NPs and Gal-siTNF-NPs against Raw 264.7 macrophages for (a) 24 h and (b) 48 h. Cell were transfected by NPs with different siTNF concentration, and subsequently treated with LPS (1 μg/mL) for 3 h. Raw 264.7 macrophages without LPS treatment were used as a negative control, and LPS-treated Raw 264.7 macrophages were used as a positive control. OF/siTNF complexes were generated according to the manufacturer's standard protocols. Each point represents the mean ± S.E.M. ($n = 3$; *$p < 0.05$, **$p < 0.01$, Student's *t*-test).

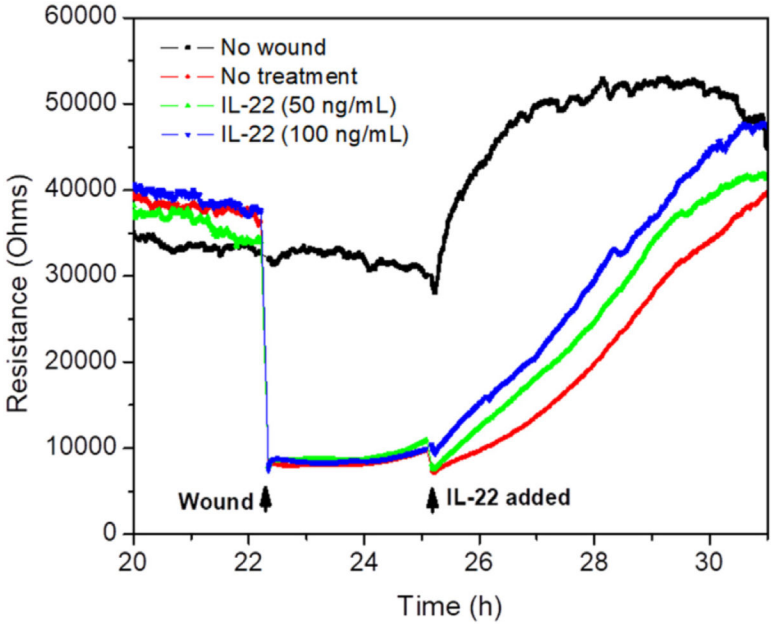

Fig. 6.

Wound healing assay of Caco2-BBE cells with the treatment of IL-22 with different concentrations (0, 50 and 100 ng/mL) on the basis of ECIS technique. 100,000 cells per well were seeded into ECIS 8W1E arrays.

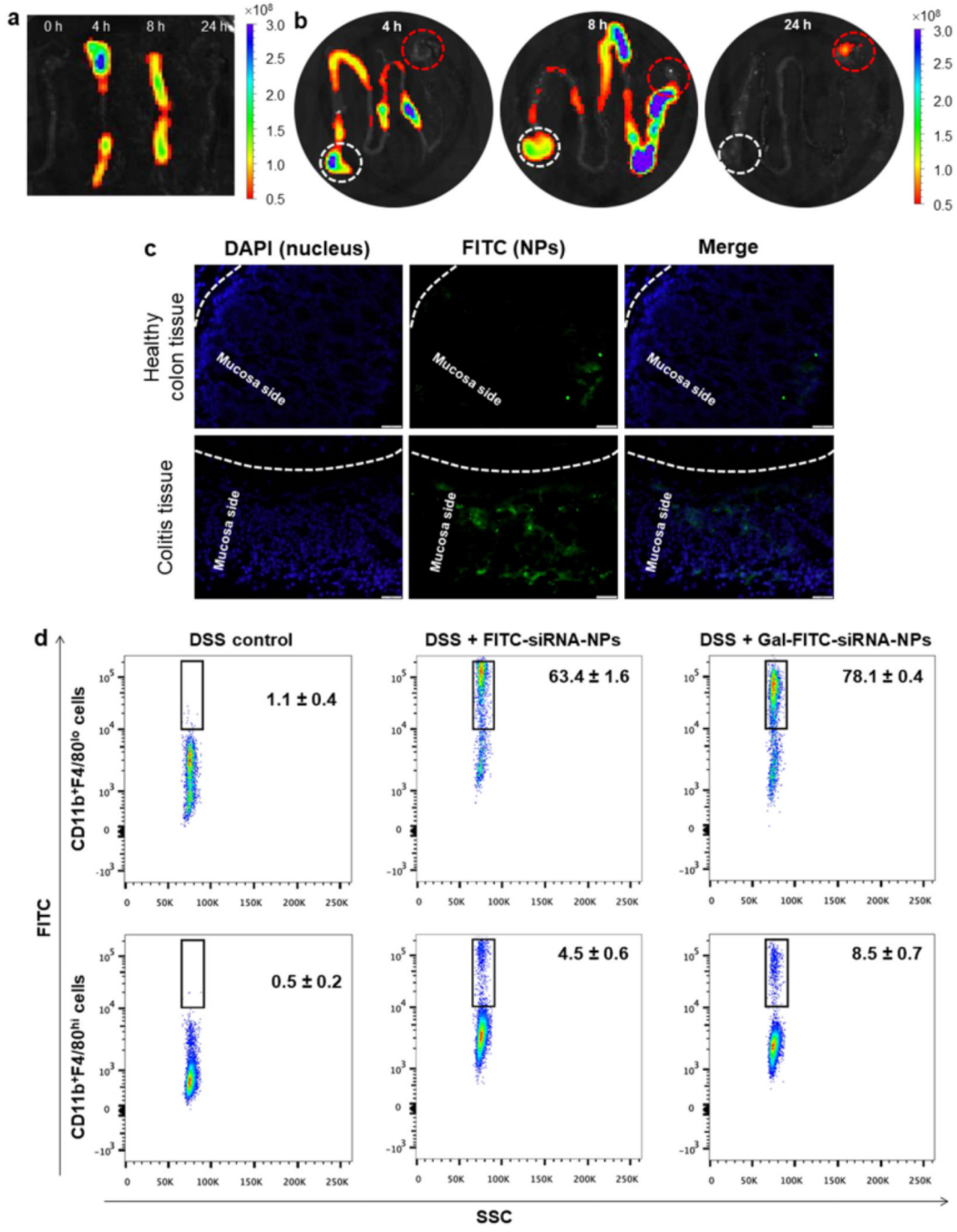

Fig. 7.

The uptake profiles of oral administered NPs by colitis tissue. Typical images of colon (a) and the rest sections of GIT (b) showing accumulation of Gal-FITC-siRNA-NPs embedded in hydrogel after oral administration in GIT at different time points (0, 4, 8 and 24 h). White dash cycle and red dash cycle in Fig. 7b indicate stomach and cecum, respectively. (c) Uptake profiles of NPs by healthy colon tissue and colitis tissue after 8 h of oral administration of Gal-FITC-siRNA-NPs embedded in hydrogel. Fixed tissues were stained with DAPI to visualize nuclei (purple). Scale bar represents 20 μm. (d) Representative FCM

analysis of FITC fluorescence-positive macrophages in mice receiving DSS and treated with hydrogel with FITC-siRNA-NPs or Gal-FITC-siRNA-NPs. Each point represents the mean ± S.E.M. (n = 3). (For interpretation of the references to colour in this figure legend, the reader is referred to the web version of this article.)

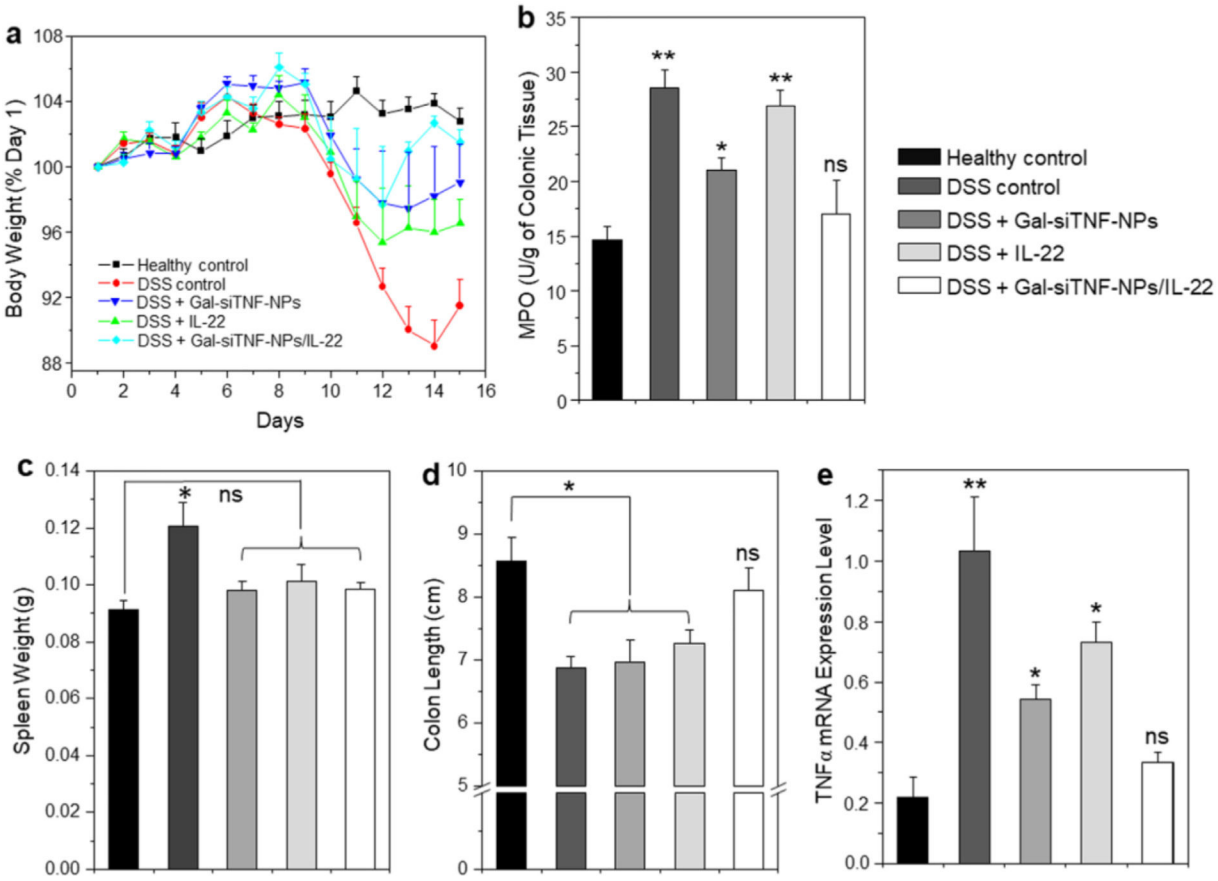

Fig. 8.

Oral administration of various drug formulations relieves DSS-induced UC in mice. (a) Mouse body weight over time, normalized as a percentage of day one body weight and given as the mean of each treatment group. (b) Colonic MPO activity, (c) spleen weight, (d) colon length and (e) TNFα mRNA expression levels in different treatment mouse groups. The MPO results are expressed as units of MPO activity per gram of tissue. Each point represents the mean ± S.E.M. ($n = 5$). Statistical significance was assessed using ANOVA followed by a Bonferroni post-test (*$p < 0.05$, **$p < 0.01$).

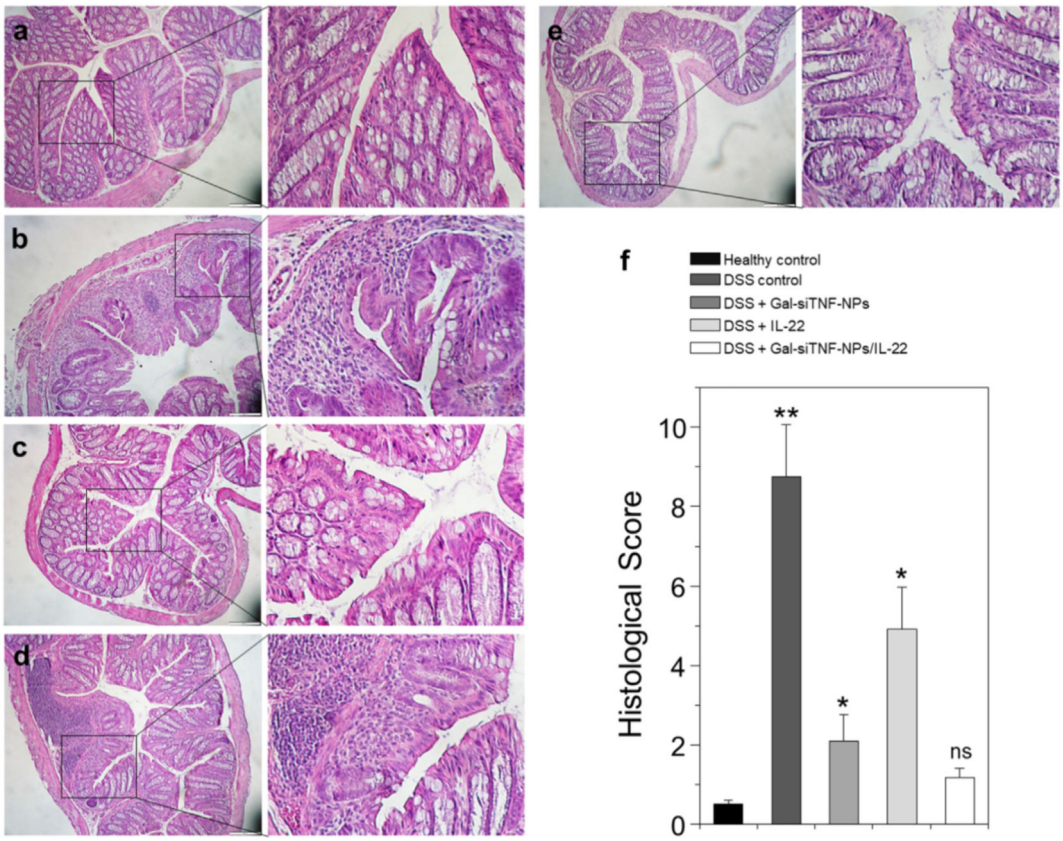

Fig. 9.

Representative H&*E*-stained colon sections from various mouse groups. (a) Healthy control mice group, (b) DSS-treated mice group, (c) Gal-siTNF-NP-treated mice group, (d) IL-22-treated mice group and (e) Gal-siTNF-NP/IL-22-treated mice group. Scale bar represents 100 μm. (f) Histological scores determined from H&E-stained colons. Each point represents the mean ± S.E.M. ($n = 3$). Statistical significance was assessed using ANOVA followed by a Bonferroni post-test (*$p < 0.05$, **$p < 0.01$).

Table 1

Characteristics of NPs (mean ± S.E.M.; $n = 3$).

Nanoparticles	Particle size (nm)	PDI	Zeta-potential (mV)	siRNA loading (ng/mg)	Encapsulation efficiency (%)
siTNF-NPs	255.7 ± 4.9	0.152	−9.5 ± 1.8	161.7 ± 11.8	61.8 ± 5.4
Gal-siTNF-NPs	261.3 ± 5.6	0.212	−6.3 ± 1.4	154.1 ± 9.7	57.2 ± 4.9